The valence band electronic structure of rhombohedral-like and tetragonal-like BiFeO$_3$ thin films from hard X-ray photoelectron spectroscopy and first-principles theory

Dipanjan Mazumdar [a], R. Knut [c,b], F. Thöle [d], M. Gorgoi [e], Sergei Faleev [f], O.N. Mryasov [f], Vilas Shelke [f], C. Ederer [d], N.A. Spaldin [d], A. Gupta [f], O. Karis [c,*]

[a] Department of Physics, Southern Illinois University, Carbondale, IL 62901, United States
[b] JILA and Department of Physics, University of Colorado Boulder and NIST, Boulder, CO 80309, USA
[c] Department of Physics and Astronomy, Uppsala University, Uppsala, Sweden
[d] Materials Theory, ETH Zürich, Wolfgang-Pauli Strasse 27, Zürich, Switzerland
[e] Helmholtz Zentrum Berlin für Materialien und Energie GmbH, BESSY II, Berlin, Germany
[f] Center for Materials for Information Technology, University of Alabama, Tuscaloosa, AL 35487, United States

ARTICLE INFO

ABSTRACT

We investigate the electronic structure of rhombohedral-like (R) and tetragonal-like (T) BiFeO$_3$ thin films using high energy X-ray photoelectron spectroscopy and first-principles electronic structure calculations. By exploiting the relative elemental cross sections to selectively probe the elemental composition of the valence band, we identify a strong Bi 6p contribution at the top of the valence band in both phases, overlapping in energy range with the O 2p states; this assignment is confirmed by our electronic structure calculations. We find that the measured occupied Bi 6p signal lies closer to the top of the valence band in the T phase than in the R phase, which we attribute, using our electronic structure calculations, to lower Bi–O hybridization in the T phase. We note, however, that our calculations of the corresponding densities of states underestimate the difference between the phases, suggesting that matrix element effects resulting from the different effective symmetries also contribute. Our results shed light on the chemical nature of the stereochemically active Bi lone pairs, which are responsible for the large ferroelectric polarization of BiFeO$_3$.

© 2015 Published by Elsevier B.V.

1. Introduction

Bismuth ferrite, BiFeO$_3$, is perhaps the most investigated multiferroic material due to its room-temperature co-existence of ferroelectricity (Curie temperature, $T_c \approx 1100$ K) and magnetism (Néel temperature, $T_N \approx 643$ K), Following the 2003 report of high ferroelectric polarization in thin films [1], a number of interesting discoveries have been made, including electrical conduction at the ferroelectric domain walls [2,3], photo-voltaic behavior [4], electric-field control of magnetism [5] and local ferroelastic switching [6,7]. A particularly intriguing effect, observed in thin-film form only, is the stabilization of a so-called "super-tetragonal" phase (T phase) under large compressive strain [8–15], which can be made to coexist with the usual rhombohedral-like structure (R phase) which

is stable at small strain values yielding so-called self-morphotropic phase boundaries [10]. Note that formally both the R and T phases are monoclinic; the rhombohedral symmetry of the bulk phase is lowered to monoclinic by the coherent heteroepitaxy even at zero strain, and ideal tetragonality can only be achieved at inaccessibly large compressive strain values [13].

In this work we investigate the valence band electronic structure of the super-tetragonal T phase and determine the similarities and differences with that of the rhombohedral-like R phase. Our study combines hard X-ray photoelectron spectroscopy (HAXPES) – chosen because it provides bulk rather than surface sensitivity [16] – with first-principles density functional theory (DFT). Since the mechanism driving ferroelectricity in BiFeO$_3$ is the stereochemically active Bi^{3+} lone pair [17,18], we focus particularly on the existence and nature of Bi 6s and 6p character in the valence band. Our measurements indicate the presence of valence band Bi 6p states in both R and T phases, with the occupied Bi 6p states in the T phase lying closer to the top of the valence band than those in the

R phase. Our density functional calculations confirm the observed presence of occupied Bi 6p states and explain their lower binding energy in the T phase in terms of reduced hybridization with O 2p states relative to the R phase. Our ground-state calculations of the differences in densities of states between the R and T phases, however, underestimate our measured differences in HAXPES spectra, suggesting that matrix element effects resulting from the different effective symmetries also play a role.

2. Experimental and computational details

100 nm-thick thin films of R-phase BiFeO$_3$ were deposited on SrRuO$_3$ buffered (40 nm) single crystal SrTiO$_3$ substrates using the pulsed laser deposition technique (248 nm, KrF excimer laser). 20 nm films of (0 0 1)-oriented T-phase BiFeO$_3$ were grown directly on LaAlO$_3$ substrates. The background oxygen pressure was kept at 100 mTorr and the deposition temperature at 700 °C for both R and T phases. Details of the sample preparation and characterization are reported elsewhere [19,20].

The HAXPES experiments were carried out on the HIKE experimental station at the KMC-1 bending magnet beamline in Helmholtz-Zentrum, Berlin. The beamline is equipped with a high resolution double crystal monochromator which consists of three sets of Si crystals [21], providing a wide range of photon energies (2–10 keV). The incident X-rays have a grazing angle relative to the sample, giving an electric field vector that is perpendicular to the sample plane. The spectrometer is mounted for detecting photoelectrons in normal emission. In the dipole approximation, this geometry strongly favors the photoionization of atomic orbitals that have out-of-plane directions, such as Bi p_z, Fe d_{z^2}, Fe d_{xz} and Fe d_{yz} [22]. The X-ray electric field vector and the measured photoelectrons are almost co-linear, which minimizes contributions from quadrupole terms in the photoionization crossection [23]. To study the different elemental contributions to the valence band, we probed a range of photon energies (2–6 keV), over which the Fe 3d and O 2p cross-sections strongly decrease with increasing photon energy such that Bi 6s and 6p are emphasized at higher photon energies. To further study the Fe 3d contributions in the valence band, we also performed resonant photoelectron spectroscopy (RPES). The RPES experiment was performed at beamline D1011 in MAX-lab, Lund. All measurements were performed at room temperature.

The structure and electronic properties of rhombohedral and tetragonal BiFeO$_3$ were calculated using first-principles density functional theory (DFT) within the local spin density approximation plus Hubbard U method (LSDA+U), as implemented in the Vienna ab initio simulation package (VASP) [24,25]. We used the Dudarev implementation of LSDA+U [26] with two U values for comparison: U_{eff} = 2 eV which was previously shown to reproduce well the bulk properties of BiFeO$_3$ [18], and U_{eff} = 5.5 eV which was shown to give a local magnetic moment on the Fe ions that is in agreement with low-temperature neutron diffraction experiments [27]. Spin–orbit coupling was included in all calculations.

3. Results and discussion

In Fig. 1 we plot the valence band structure measured by HAXPES at photon energies of 2100, 3000 and 6000 eV for both the T (solid lines) and R (dashed lines) phases. For both structures, and for all photon energies, we observe a localized peak between 11 and 14 eV binding energy (see dashed line C in Fig. 1) that arises predominantly from Bi 6s states and is almost unchanged between the R and T phases. The broad peak between 2 and 9 eV binding energy observed in both polymorphs is generally attributed to hybridized Fe 3d–O 2p states with a considerable amount of Bi 6p character [18]; this peak shows qualitative differences between the
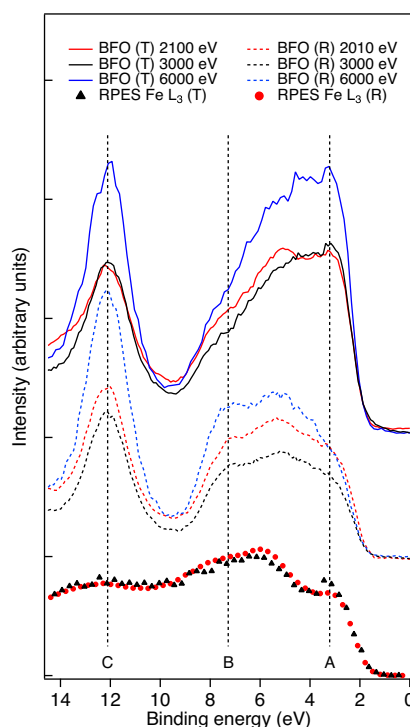

Fig. 1. Valence band spectra of BiFeO$_3$ at photon energies of 2100, 3000 and 6000 eV, for both T and R phase with solid and dotted lines, respectively. RPES for T phase and R phase are shown with triangles and circles, respectively.

R and T phases which we discuss later. Additional narrow peaks are found at binding energies of 26 eV and 29 eV (not shown), which we attribute to spin–orbit split Bi 5$d_{5/2}$ and Bi 5$d_{3/2}$ core levels, respectively. All the valence band spectra have been normalized so that the intensity of the Bi 5$d_{5/2}$ state is the same.

To help interpret our data, in Fig. 2 we show literature values of the cross sections, with the asymmetry parameter included, of various valence band states [28,23,29] relative to the Bi 5$d_{5/2}$ states; this corresponds to the normalization used in Fig. 1. Fig. 2 illustrates the established result that both Fe and O contributions show a strong decrease in cross section with increasing photon energy while Bi states show a strong increase. In our measurements, we find that the intensity of the valence band photoemission increases significantly at higher incident photon energy for both R and T phases. Based on the energy dependence of the cross sections shown in Fig. 2, this suggests a considerable Bi contribution in the valence
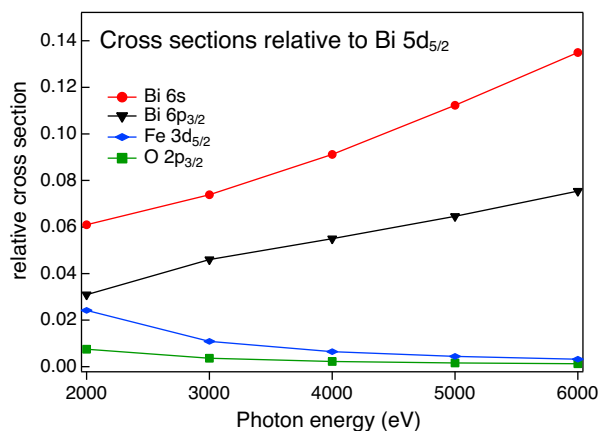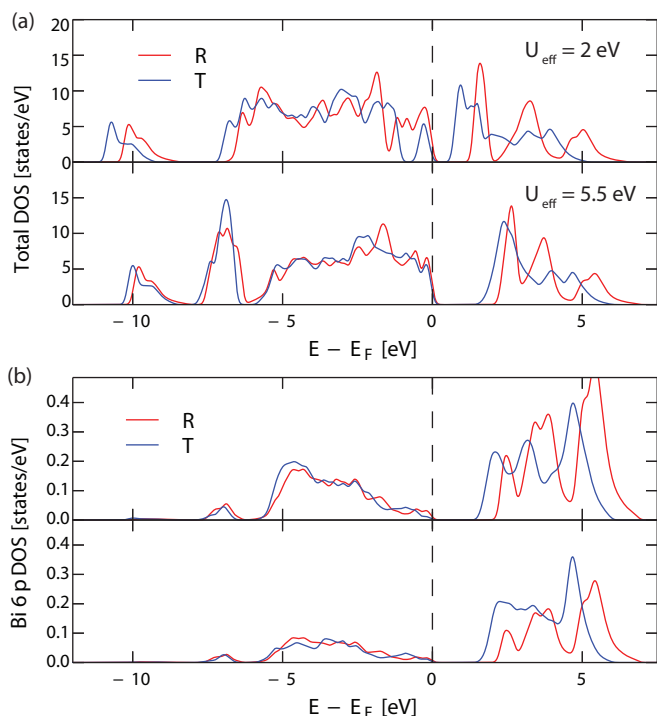

Fig. 2. Atomic cross section of various core levels relative to the Bi 5d core level (normalized to the Bi 5d values) as a function of photon energy. From Ref. [28,23,29].

Fig. 3. (a) Calculated total densities of states for T and R phase BiFeO₃. The upper panel corresponds to $U_{eff} = 2$ eV, the lower panel corresponds to $U_{eff} = 5.5$ eV. (b) Calculated orbital-resolved densities of states (with $U_{eff} = 5.5$ eV) for the in-plane (upper panel) and out-of-plane (lower panel) Bi 6p orbitals in T and R phase BiFeO₃. The axes for the projected orbitals correspond to the pseudocubic directions.

Table 1

Experimental (HAXPES), obtained from 6 keV data, the and calculated (DFT) centroids of the occupied Bi 6p states. The numbers are obtained by integration over the bands in the energy window from −9 eV to the valence band top at 0 eV. The calculated centroids of the unoccupied Bi 6p bands are also shown for comparison, integrated from 0 to 8 eV. The trends in experimental and calculated $6p_z$ centroids are similar.

		Occupied (eV)	Unoccupied (eV)
HAXPES	R	−5.6	–
	T	−4.9	–
DFT out-of-plane ($6p_z$)	R	−3.87	4.35
	T	−3.61	3.84
DFT in-plane ($6p_x + 6p_y$)	R	−3.93	4.33
	T	−4.16	4.03

thus conclude that $U = 5.5$ eV is a more appropriate value and use it in our further analysis.

First we quantify the average position of the occupied Bi $6p_z$ states by calculating the centroids of the respective bands in both R and T phases. Consistent with our XPS data, we find that the Bi $6p_z$ centroid is closer to the valence band top in the T phase than in the R phase (Table 1) when $U_{eff} = 5.5$ eV is used. Interestingly, smaller or larger values of U_{eff} do not reproduce this effect, providing further support for the choice of 5.5 eV. We find also that the unoccupied Bi p_z states are lower in energy on average in the T phase, indicating that the change in valence band Bi p character is consistent with a reduced interaction between Bi p_z and O 2p in the T phase giving less bonding–anti-bonding splitting. Note that the occupied in-plane $6p_x$ and $6p_y$ orbitals, which our experiments are not sensitive to, have the opposite calculated behavior, and are at lower energy (further from the valence band edge) in the T phase than in the R phase.

The qualitative shape of the occupied Bi 6p density of states, Fig. 3(b) (as well as their total occupation, obtained from the integrated partial density of states up to the Fermi energy), does not show any substantive changes between R and T phase. The measured change in shape is therefore likely due to matrix element effects. This is notable since, as mentioned previously, the two phases formally have the same monoclinic symmetry.

4. Summary

To summarize, we have used HAXPES and DFT to study the bulk electronic structure of rhombohedral and tetragonal BiFeO₃ thin films. We find a considerable occupation of Bi 6p states within the valence band, consistent with the known stereochemical activity of the Bi lone pair. We find a significant difference in the nature of the occupied states near the valence band top for the two phases, which we assign to be Bi $6p_z$ states by considering both the relative cross sections and the geometry of the experimental setup. Our DFT calculations qualitatively show the same trend as our XPS data, and offer an explanation for the binding energy differences in terms of lower Bi–O hybridization in the tetragonal structure. This is corroborated by RPES measurements which indicate that the Fe 3d states are substantially similar in the two phases.

band density of states. We also observe that the valence band shows higher intensity at low binding energy in the T phase than in the R phase indicating a larger contribution of Bi 6p states near the valence band top in T-phase than in R-phase BiFeO₃.

In Fig. 1 we also show the RPES spectrum obtained at the photon energy corresponding to the Fe L_3 absorption edge, in order to strongly enhance the Fe 3d contribution in the valence band [30]. The RPES Fe L_3 spectra for both R and T phases are very similar, with both showing features close to the valence band edge and 4 eV below (vertical dashed lines A and B respectively in Fig. 1). This indicates that the difference in valence band structure between the R and T phases is mainly due to changes in Bi 6p hybridized states.

In Fig. 3 we show our calculated total and orbital-resolved Bi 6p densities of states for both structural polymorphs at two different values of the U parameter (2 and 5.5 eV). In order to facilitate comparisons to the experimental results, the calculated densities of states are smoothed with a Gaussian kernel with a bandwidth of 0.1 eV.

Our calculations confirm the assignment of the peak at −10 eV to Bi 6s states. As discussed previously [18], the broad band near the Fermi energy is composed largely of O 2p and Fe 3d character. However, we also find a considerable Bi 6p contribution, consistent with our HAXPES data and the model of lone pairs contributing to stereochemical activity through admixture of cation p states [17,31].

The upper panel of Fig. 3 shows the total DOS calculated using $U_{eff} = 2$ eV. At this U value we obtain a split-off occupied Fe d band separated by a gap from the rest of the valence band. This situation is not confirmed by the RPES results in Fig. 1 indicating that the LDA+U method with $U = 2$ eV does not completely capture the physics of T-phase BiFeO₃. On increasing U_{eff} to 5.5 eV (lower panel in Fig. 3(a)), however, the gap closes and the previously split-off band is no longer separated from the rest of the valence band. We

References

[1] J. Wang, J.B. Neaton, H. Zheng, V. Nagarajan, S.B. Ogale, B. Liu, D. Viehland, V. Vaithyanathan, D.G. Schlom, U.V. Waghmare, N.A. Spaldin, K.M. Rabe, M. Wuttig, R. Ramesh, Epitaxial BiFeO$_3$ multiferroic thin film heterostructures, Science 299 (5613) (2003) 1719–1722.

[2] J. Seidel, L.W. Martin, Q. He, Q. Zhan, Y.H. Chu, A. Rother, M.E. Hawkridge, P. Maksymovych, P. Yu, M. Gajek, N. Balke, S.V. Kalinin, S. Gemming, F. Wang, G. Catalan, J.F. Scott, N.A. Spaldin, J. Orenstein, R. Ramesh, Conduction at domain walls in oxide multiferroics, Nat. Mater. 8 (3) (2009) 229–234, http://dx.doi.org/10.1038/NMAT2373.

[3] P. Maksymovych, J. Seidel, Y.H. Chu, P. Wu, A.P. Baddorf, L.-Q. Chen, S.V. Kalinin, R. Ramesh, Dynamic conductivity of ferroelectric domain walls in BiFeO$_3$, Nano Lett. 11 (5) (2011) 1906–1912, http://dx.doi.org/10.1021/nl104363x.

[4] T. Choi, S. Lee, Y.J. Choi, V. Kiryukhin, S.W. Cheong, Switchable ferroelectric diode and photovoltaic effect in BiFeO$_3$, Science 324 (5923) (2009) 63–66, http://dx.doi.org/10.1126/science.1168636.

[5] T. Zhao, A. Scholl, F. Zavaliche, K. Lee, M. Barry, A. Doran, M.P. Cruz, Y.H. Chu, C. Ederer, N.A. Spaldin, R.R. Das, D.M. Kim, S.H. Baek, C.B. Eom, R. Ramesh, Electrical control of antiferromagnetic domains in multiferroic BiFeO$_3$ films at room temperature, Nat. Mater. 5 (10) (2006) 823–829, http://dx.doi.org/10.1038/nmat1731.

[6] N. Balke, S. Choudhury, S. Jesse, M. Huijben, Y.H. Chu, A.P. Baddorf, L.Q. Chen, R. Ramesh, S.V. Kalinin, Deterministic control of ferroelastic switching in multiferroic materials, Nat. Nanotechnol. 4 (12) (2009) 868–875, http://dx.doi.org/10.1038/NNANO.2009.293.

[7] S.H. Baek, H.W. Jang, C.M. Folkman, Y.L. Li, B. Winchester, J.X. Zhang, Q. He, Y.H. Chu, C.T. Nelson, M.S. Rzchowski, X.Q. Pan, R. Ramesh, L.Q. Chen, C.B. Eom, Ferroelastic switching for nanoscale non-volatile magnetoelectric devices, Nat. Mater. 9 (4) (2010) 309–314, http://dx.doi.org/10.1038/NMAT2703.

[8] K.Y. Yun, D. Ricinschi, T. Kanashima, M. Noda, M. Okuyama, Giant ferroelectric polarization beyond 150 mu c/cm(2) in BiFeO$_3$ thin film, Jpn. J. Appl. Phys. Part 2 - Lett. Express Lett. 43 (5A) (2004) L647–L648, http://dx.doi.org/10.1143/JJAP.43.L647.

[9] D. Ricinschi, K.Y. Yun, M. Okuyama, A mechanism for the 150 μC cm^{-2} polarization of BiFeO$_3$ films based on first-principles calculations and new structural data, J. Phys.: -Condes. Matter 18 (6) (2006) L97–L105, http://dx.doi.org/10.1088/0953-8984/18/6/L03.

[10] R.J. Zeches, M.D. Rossell, J.X. Zhang, A.J. Hatt, Q. He, C.H. Yang, A. Kumar, C.H. Wang, A. Melville, C. Adamo, G. Sheng, Y.H. Chu, J.F. Ihlefeld, R. Erni, C. Ederer, V. Gopalan, L.Q. Chen, D.G. Schlom, N.A. Spaldin, L.W. Martin, R. Ramesh, A strain-driven morphotropic phase boundary in BiFeO$_3$, Science 326 (5955) (2009) 977–980, doi:10.1126/science.1177046.

[11] H. Bea, B. Dupe, S. Fusil, R. Mattana, E. Jacquet, B. Warot-Fonrose, F. Wilhelm, A. Rogalev, S. Petit, V. Cros, A. Anane, F. Petroff, K. Bouzehouane, G. Geneste, B. Dkhil, S. Lisenkov, I. Ponomareva, L. Bellaiche, M. Bibes, A. Barthelemy, Evidence for room-temperature multiferroicity in a compound with a giant axial ratio, Phys. Rev. Lett. 102 (21) (2009), http://dx.doi.org/10.1103/PhysRevLett.102.217603.

[12] D. Mazumdar, V. Shelke, M. Iliev, S. Jesse, A. Kumar, S.V. Kalinin, A.P. Baddorf, A. Gupta, Nanoscale switching characteristics of nearly tetragonal BiFeO$_3$ thin films, Nano Lett. 10 (7) (2010) 2555–2561, http://dx.doi.org/10.1021/nl101187a.

[13] H.M. Christen, J.H. Nam, H.S. Kim, A.J. Hatt, N.A. Spaldin, Stress-induced r-m-a-m-c-t symmetry changes in BiFeO$_3$ films, Phys. Rev. B 83 (14) (2011), http://dx.doi.org/10.1103/PhysRevB.83.144107.

[14] O. Dieguez, O.E. Gonzalez-Vazquez, J.C. Wojdel, J. Iniguez, First-principles predictions of low-energy phases of multiferroic BiFeO$_3$, Phys. Rev. B 83 (9) (2011), http://dx.doi.org/10.1103/PhysRevB.83.094105.

[15] P. Chen, N.J. Podraza, X.S. Xu, A. Melville, E. Vlahos, V. Gopalan, R. Ramesh, D.G. Schlom, J.L. Musfeldt, Optical properties of quasi-tetragonal BiFeO$_3$ thin films, Appl. Phys. Lett. 96 (13) (2010), http://dx.doi.org/10.1063/1.3364133.

[16] G. Panaccione, K. Kobayashi, Hard X-ray photoemission spectroscopy: Variable depth analysis of bulk, surface and interface electronic properties, Surf. Sci. 606 (3–4) (2012) 125–129, http://dx.doi.org/10.1016/j.susc.2011.10.022.

[17] R. Seshadri, N.A. Hill, Visualizing the role of bi 6s "lone pairs" in the off-center distortion in ferromagnetic BiMnO$_3$, Chem. Mat. 13 (9) (2001) 2892–2899, http://dx.doi.org/10.1021/cm010090m.

[18] J.B. Neaton, C. Ederer, U.V. Waghmare, N.A. Spaldin, K.B. Rabe, First-principles study of spontaneous polarization in multiferroic BiFeO$_3$, Phys. Rev. B 71 (1) (2005), http://dx.doi.org/10.1103/PhysRevB.71.014113.

[19] V. Shelke, V.N. Harshan, S. Kotru, A. Gupta, Effect of kinetic growth parameters on leakage current and ferroelectric behavior of BiFeO$_3$ thin films, J. Appl. Phys. 106 (10) (2009), http://dx.doi.org/10.1063/1.3254190.

[20] V. Shelke, D. Mazumdar, G. Srinivasan, A. Gupta, The role of SrRuO$_3$ bottom layer in strain relaxation of BiFeO$_3$ thin films deposited on lattice mismatched substrates, J. Appl. Phys. 109 (7) (2011), http://dx.doi.org/10.1063/1.3564940.

[21] S. Granroth, W. Olovsson, E. Holmström, R. Knut, M. Gorgoi, S. Svensson, O. Karis, Understanding interface properties from high kinetic energy photoelectron spectroscopy and first principles theory, J. Electron Spectrosc. Relat. Phenom. 183 (1–3) (2011) 80–93, http://dx.doi.org/10.1016/j.elspec.2010.08.004.

[22] C.R. Brundle, A.D. Baker, Electron Spectroscopy: Theory, Techniques and Applications, vol. 2, Academic Press, London, 1978.

[23] M.B. Trzhaskovskaya, V.I. Nefedov, V.G. Yarzhemsky, Photoelectron angular distribution parameters for elements $z = 1$ to $z = 54$ in the photoelectron energy range 100–5000 eV, Atom. Data Nucl. Data Tables 77 (1) (2001) 97–159.

[24] G. Kresse, J. Hafner, Abinitio molecular-dynamics for liquid-metals, Phys. Rev. B 47 (1) (1993) 558–561.

[25] G. Kresse, J. Furthmüller, Efficient iterative schemes for ab initio total-energy calculations using a plane-wave basis set, Phys. Rev. B 54 (16) (1996) 11169–11186.

[26] S.L. Dudarev, G.A. Botton, S.Y. Savrasov, C.J. Humphreys, A.P. Sutton, Electron-energy-loss spectra and the structural stability of nickel oxide: an LSDA + U study, Phys. Rev. B 57 (3) (1998) 1505–1509.

[27] P. Fischer, M. Polomska, I. Sosnowska, M. Szymanski, Temperature-dependence of the crystal and magnetic-structures of BiFeO$_3$, J. Phys. C Solid State 13 (10) (1980) 1931–1940.

[28] J. Scofield, Theoretical photoionization cross sections from 1 to 1500 keV, Tech. Rep. UCRL-51326, Lawrence Livermore National Laboratory Rep, 1973.

[29] M.B. Trzhaskovskaya, V.I. Nefedov, V.G. Yarzhemsky, Photoelectron angular distribution parameters for elements $z = 55$ to $z = 100$ in the photoelectron energy range 100–5000 eV, Atom. Data Nucl. Data Tables 82 (2) (2002) 257–311, http://dx.doi.org/10.1006/adnd.2002.0886.

[30] P.A. Brühwiler, O. Karis, N. Mårtensson, Charge-transfer dynamics studied using resonant core spectroscopies, Rev. Mod. Phys. 74 (3) (2002) 703–740.

[31] U.V. Waghmare, N.A. Spaldin, H.C. Kandpal, R. Seshadri, First-principles indicators of metallicity and cation off-centricity in the IV-VI rocksalt chalcogenides of divalent Ge, Sn, and Pb, Phys. Rev. B 67 (12) (2003), http://dx.doi.org/10.1103/PhysRevB.67.125111.